J. Phys. 56, 381 (1978).

[4]B. H. Ripin, F. C. Young, J. A. Stamper, C. M. Armstrong, R. Decoste, E. A. McLean, and S. E. Bodner, Phys. Rev. Lett. 39, 611 (1977).

[5]B. H. Ripin, J. M. McMahon, E. A. McLean, W. M. Manheimer, and J. A. Stamper, Phys. Rev. Lett. 33,

634 (1974).

[6]R. Massey, K. Berggren, and A. Z. Pietryzk, Phys. Rev. Lett. 36, 963 (1976).

[7]J. F. Drake, P. K. Kaw, Y. C. Lee, G. Schmidt, C. S. Liu, and Marshall N. Rosenbluth, Phys. Fluids 17, 778 (1974).

Self-Magnetic-Field Generation in a Plasma

S. P. Obenschain[a] and N. C. Luhmann, Jr.
University of California, Los Angeles, California 90024
(Received 19 July 1978)

Experimental results are presented on the growth, diffusion, and saturation of magnetic fields spontaneously generated by the interaction of intense microwave radiation with an inhomogeneous plasma. Finite-bandwidth pumps permitted the investigation of the mechanisms responsible for magnetic field generation and their control.

Megagauss dc magnetic fields which have been observed in experiments with laser-irradiated solid targets[1,2] may play an important role in both energy absorption and transport in laser-irradiated–pellet fusion. Several mechanisms for magnetic-field generation have been proposed[3,4] including resonance absorption and nonparallel temperature and density gradients.

The short temporal and spatial scales in laser experiments make detailed measurements of these magnetic fields difficult. Herein we report on experiments employing microwaves in large tenuous plasmas where precise measurements can be made more easily. An earlier experiment by DiVergilio *et al.*[5] demonstrated the feasibility of magnetic field generation in such a device. We have investigated the growth and saturation of self-generated magnetic fields over five-orders-of-magnitude variation in incident field intensity. In addition, we have investigated the effects of finite-bandwidth pumps on magnetic field generation.

Microwave radiation ($f_0 \simeq 3$ GHz) is launched from a gridded horn (aperture $\simeq 2\lambda_0$) along the z axis of a cylindrical unmagnetized plasma (60 cm diam, 80 cm length) produced by a multifilament discharge. The plasma density increases along z ($n|dn/dz|^{-1} \simeq 50$ cm $\simeq 5\lambda_0$). There is also a relatively gentle density gradient parallel to the incident electric field E_x ($n|dn/dx|^{-1} \simeq 200$ cm). To minimize accentuation of axial field components due to wave refraction in the plasma, the experiments are conducted with the critical-den-

sity surface located within a few vacuum wavelengths of the horn aperture. Typical plasma parameters are $T_e/T_i \approx 10$, $T_e \approx 3$ eV, and $n_n \approx 10^{13}$ cm^{-3}. The calculated value for $\eta_{\text{vac}} = E_{\text{vac}}^2/8nkT_e$ is approximately 1% at an incident power of 2.4 kW. For the experiments reported herein $10^{-5} \lesssim \eta_{\text{vac}} \lesssim 1$.

A variety of interactions occur in the vicinity of the critical layer shortly after the onset of microwave pulses of typical rise time $\tau \simeq 10$ nsec. We observe density steepening near the critical layer, electron main-body heating, the appearance of ion waves, exponentially growing high-frequency fields characteristic of parametric instability, and the acceleration of the tail of the electron distribution. In addition, we observe the growth and diffusion of magnetic fields in the plasma. The magnetic fields are measured using axially and radially movable 1-cm-diam, 10-turn electrostatically shielded coils. The measured time response of these coils is < 20 nsec in vacuum. The axial component of the magnetic field B_z is parallel to the horn and plasma chamber axis, while B_y is perpendicular to the incident linearly polarized microwave electric field. B_y was consistently the largest field component.

Figure 1 shows the growth of B_y near the axis as a function of axial position at a moderate power level ($\eta_{\text{vac}} \simeq 10^{-3}$). The rf was turned on at $t = 0$ and remained on for the times indicated. Radial measurements indicate that the field is apparently formed by currents parallel to E_x flowing within a few centimeters of the critical lay-
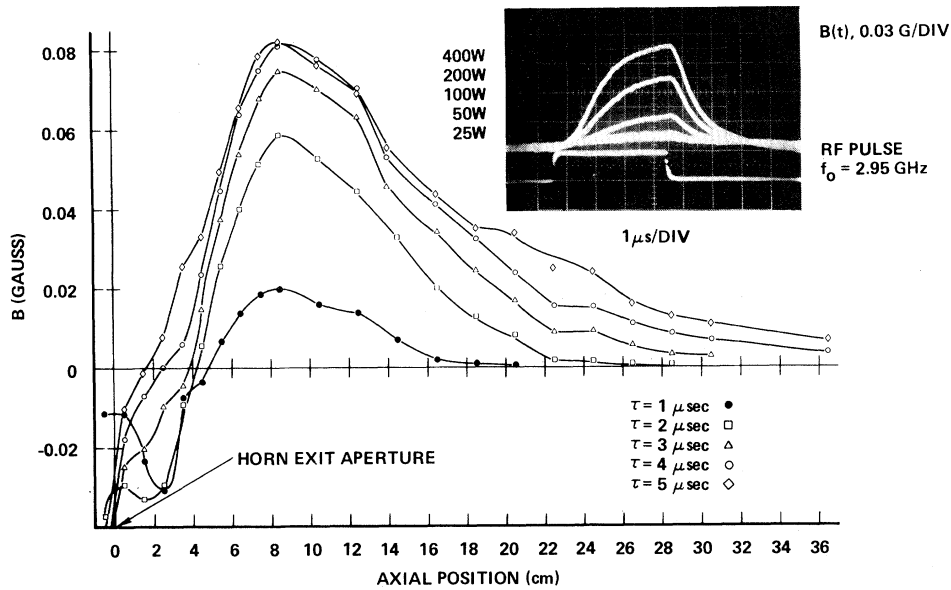
FIG. 1. Axial variation of B_y at intervals from 1–5 μsec after rf onset. The critical layer is located approximately at z = 5 cm.

er. Note that the field null point monotonically propagates into the underdense plasma. The magnetic field diffuses at a rate consistent with the calculated plasma resistivity. Upon cessation of rf input, the magnetic fields persist for several microseconds, decaying at a rate consistent with their spatial extent and the plasma resistivity (see Fig. 1 inset).

At the relatively low power level which the results of Fig. 1 represent, the measured main-body heating is too small to account for the observed field amplitude through the $\nabla n \times \nabla T$ source term. Moreover, since the heating peaks on axis ($r \simeq 0$) near the critical layer and ∇n is nearly axial, the field produced by this term should be toroidal about the z axis. In contrast, our experiments indicate that near the critical layer, the fields are produced by currents parallel to E_x as one would expect for field generation due to resonance absorption.

The growth of the magnetic field as a function of power was investigated. At moderate power levels ($\eta_{vac} \lesssim 10^{-2}$) the magnetic field in the overdense and underdense plasma well removed (by a few centimeters) from the critical-density layer monotonically increases in amplitude to a saturated value which remains constant for the longest microwave pulses ($\simeq 15$ μsec) employed. The saturated magnitude of B_y in the overdense plasma is displayed in Fig. 2(a) as a function of power. At very low powers ($P < 50$ W, $\eta_{vac} < 2$

$\times 10^{-4}$) the magnetic field increases nearly linearly with incident power. There is no clearly discernible threshold for the appearnce of the magnetic field. In this regime, the early growth rates approximately agree with predictions concerning magnetic field generation due to resonance absorption. The initial growth rate near the critical layer is given by[6]

$$\dot{B}_y \approx A(\pi e/mc)\eta(nkT_e)\sin\theta\cos\theta,$$

where A is the absorption coefficient and θ is the angle of incidence. Using $\theta \simeq 14°$ as determined by axial electric-field measurements together with the density scale length to compute the expected absorption coefficient in a linear density profile, one obtains $\dot{B}_y \approx 2.5 \times 10^{-4}$ G/μsec for an incident power level of 50 W. This compares well with the experimentally measured value of 4×10^{-4} G/μsec. The linear relationship between the saturated magnetic field and input power agrees with theoretical predictions of magnetic field strength limited by wave convection or diffusion of the magnetic field from the source region. However, the saturation time (≈ 1.5 μsec) and the saturated level are approximately an order of magnitude larger than theoretical predictions.[6]

At powers in excess of approximately 50 W there is a sharp break in the curve of saturated field versus power together with a sudden increase in saturation time. The saturated field
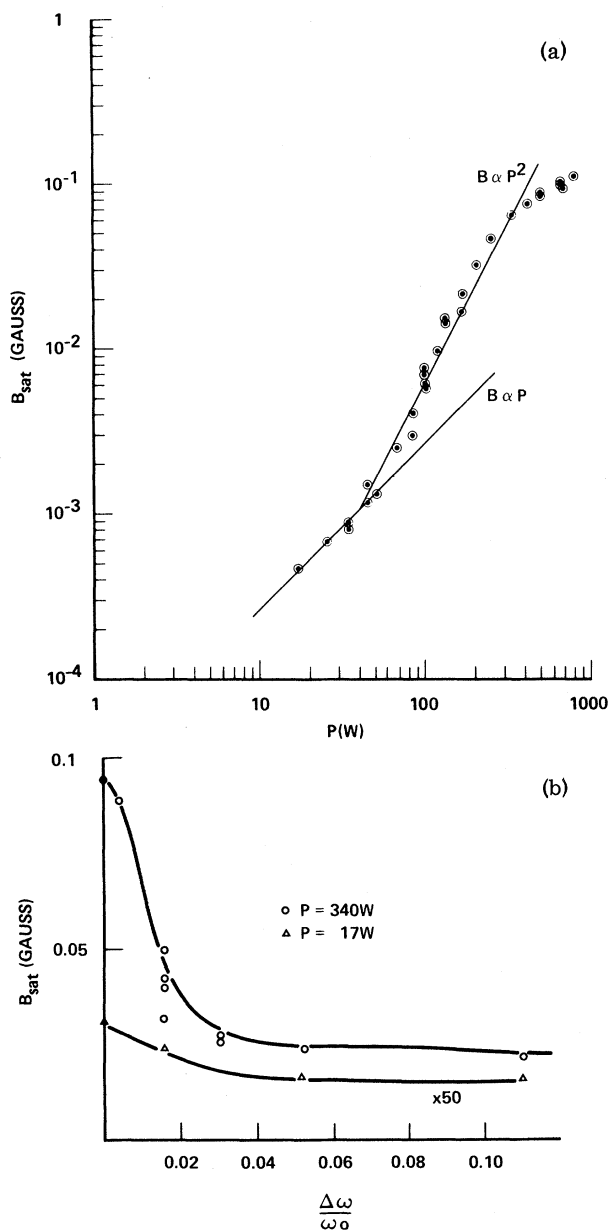
FIG. 2. (a) B_{sat} vs incident power for $\eta_{vac} < 5 \times 10^{-3}$. (b) B_{sat} vs pump bandwidth for $\eta_{vac} = 7 \times 10^{-5}$ and 1.4×10^{-3}.

increases more nearly as P^2 for powers in the range of 50 to 300 W. At 50-W incident power, the magnetic field grows and saturates within 1.5 μsec. At 80 W the growth is bimodal, with the magnetic field increasing rapidly to approximately half its saturated value during the first 1.5 μsec, and the field more slowly increasing to its full saturated value in approximately 7 μsec. At higher power levels the saturation time de-

creases to $\simeq 2$ μsec. This behavior is consistent with the onset of parametric instability. Near threshold, the parametric decay reaches saturation relatively slowly, while the saturation time decreases at higher intensities. The P^2 dependence of B can be explained through the power-dependent absorption coefficient.

We have further investigated the spatial and temporal evolution of B_y at high intensities ($\eta_{vac} \simeq 0.1$) using short-duration pulses ($\simeq 200$ nsec) in order to reduce the effects of both parametric instability and the $\nabla n \times \nabla T$ source. The magnetic field at $\simeq 100$ nsec after the beginning of the pulse is found to be quite localized ($k_0 \Delta x \simeq 2$ at full width at half maximum) as is expected for resonance absorption. However, the width increases rapidly (doubling during the next 100 nsec) presumably a result of the increasing importance of other source and loss terms.

In previous experiments,[7,8] the effect of finite pump bandwidth on parametric instability, density-profile modification, and hot-electron production was examined. It was found that a randomly modulated pump with a bandwidth exceeding several percent attentuated or eliminated the above phenomena. Similarly, one would expect that the magnetic field due to resonant phenomena such as parametric instability should exhibit significant reduction when a finite-bandwidth pump is employed. However, the actual effects will be sensitively dependent upon the particular resonant phenomenon. For example, resonance absorption is a linear process which can occur at different frequencies at different locations along a plasma density gradient and thus can be relatively unaffected by moderate bandwidths in contrast to the parametric instability.

The saturated level of B_y as a function of pump bandwidth is shown in Fig. 2(b) at two power levels. The higher power (340 W) is located just above the region where the magnetic field is a very rapidly increasing function of power, while the lower power is located in the linear regime ($B \propto P$). At the higher power, bandwidths $\Delta \omega / \omega_0$ as small as 1% yielded significant reduction in the magnetic field. The magnetic field was nearly independent of bandwidth for $\Delta \omega / \omega_0 > 3\%$. Small bandwidths apparently eliminate the field produced by phenomena such as the parametric decay instability which are sensitive to pump bandwidth. The residual field unaffected by pump bandwidth may be due to simple resonance absorption. At a lower power level ($P \simeq 17$ W), finite bandwidth has a much smaller effect on the mag-

netic field generation. The above results were obtained using randomly modulated pumps and appeared to be independent of whether the pump-bandwidth mechanism was due to random phase or amplitude modulation.

For $P \gtrsim 2$ kW, the magnetic field does not simply saturate, but exhibits a more complicated temporal behavior even at locations well removed from the critical layer. Figure 3 shows the magnitude of B_y as a function of incident power at several times after pump turnon. When measured during the first few microseconds, B_y is a monotonically increasing function of pump power. However, when measured at successively later times, B_y begins to decrease with increasing power. This effect is very pronounced for $\eta_{vac} \gtrsim 5 \times 10^{-2}$. We note that at these high power levels, there are large, relatively complex, density-profile modifications due to radiation pressure which follow approximately the interference pattern of the incident and reflected rf pulse.[9] In addition, at the higher powers, some ionization occurs for larger pulse durations. Such density-profile changes could modify the efficiency of resonance absorption as well as other magnetic-field-generation mechanisms.

Magnetic field generation using short duration (1.5 μsec) very-high-power pulses ($\eta_{vac} \lesssim 1$) was also investigated. For these pulses, the peak magnetic field remains a monotonically increasing function of incident power. In the range 2 kW $\lesssim P \lesssim 20$ kW, the B field increases nearly linearly with $P^{1/2}$. For $\eta_{vac} \gtrsim 0.1$, B increases more slowly than $P^{0.25}$. For $P \gtrsim 2$ kW, electron mainbody heating ΔT_e is observed which is sufficiently large for the $\nabla n \times \nabla T$ term to be significant. For $\eta_{vac} \lesssim 0.1$, $\nabla T_e \propto P$. It is interesting to note that the increase of ΔT_e with increasing P begins to saturate at approximately the same power at which the saturation of B occurs.

The present investigations indicate that the generation of magnetic fields even in the relatively simple geometry of our experimental arrangement is a complicated, multimechanism process. The measurements of the saturated field as a function of power provide a comparison for theoretical treatments accounting for multimechanism generation and diffusion of B fields.

We would like to thank G. Huffman of Varian Associates and J. Quinn of EIMAC for their gen-
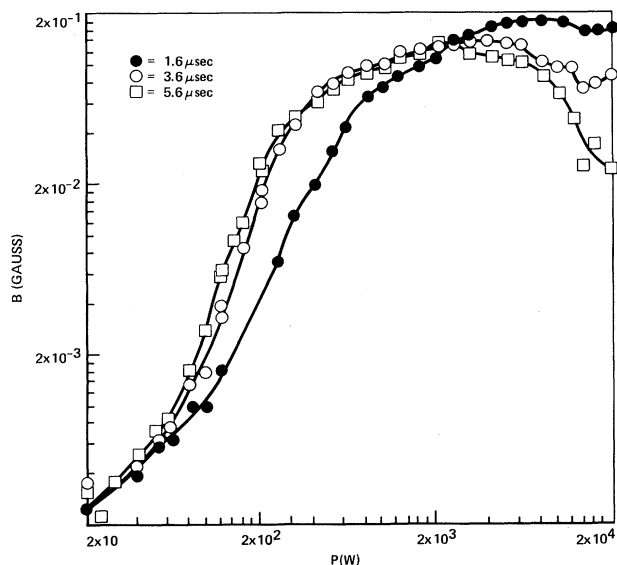
FIG. 3. B vs incident power at intervals from 1 to 6 μsec after rf onset.

erous assistance which made these studies possible. This was supported in part by the Office of Laser Fusion, U. S. Department of Energy Contract No. EY-76-S-03-0034 PA 236 and U. S. Air Force Office of Scientific Research Contract No. F49620-76-C-0012.

[a] Present address: Naval Research Laboratory, Washington, D. C. 20375.

[1] J. A. Stamper, K. Papadopoulos, R. N. Sudan, S. O. Dean, E. A. McLean, and J. M. Dawson, Phys. Rev. Lett. 26, 1012 (1971).

[2] J. A. Stamper, E. A. McLean, and B. H. Ripin, Phys. Rev. Lett. 40, 1177 (1978).

[3] D. G. Colombant and N. K. Winsor, Phys. Rev. Lett. 38, 697 (1977).

[4] J. J. Thomson, C. E. Max, and K. Estabrook, Phys. Rev. Lett. 35, 663 (1975).

[5] W. F. DiVergilio, A. Y. Wong, H. C. Kim, and Y. C. Lee, Phys. Rev. Lett. 38, 541 (1977).

[6] T. Speziale and P. J. Catto, Phys. Fluids 21, 2063 (1978).

[7] S. P. Obenschain, N. C. Luhmann, Jr., and P. T. Greiling, Phys. Rev. Lett. 36, 1309 (1976).

[8] S. P. Obenschain and N. C. Luhmann, Jr., Appl. Phys. Lett. 30, 452 (1977).

[9] Y. Nishida, N. C. Luhmann, Jr., and S. P. Obenschain, Bull. Am. Phys. Soc. 23, 886 (1978).
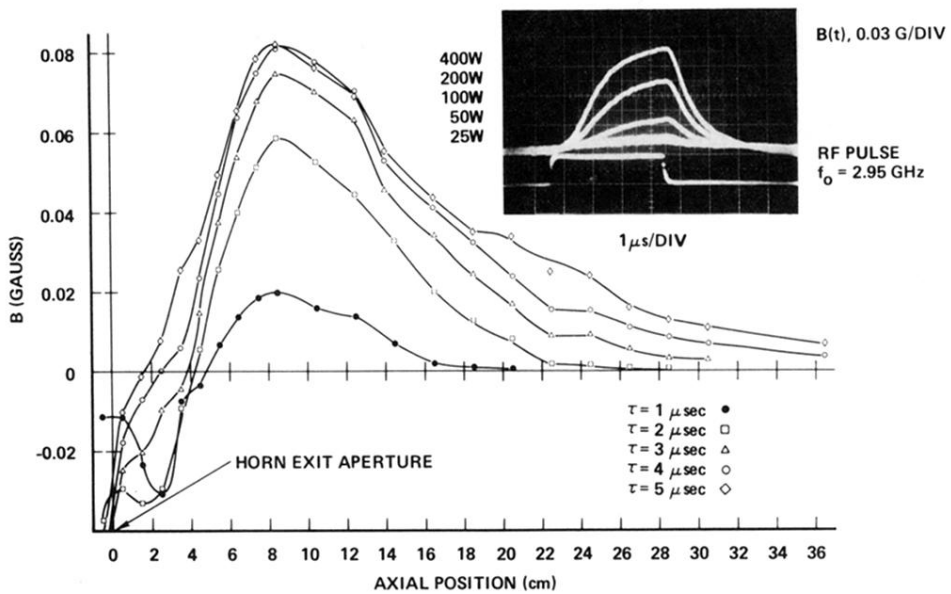
FIG. 1. Axial variation of B_y at intervals from $1-5\,\mu$sec after rf onset. The critical layer is located approximately at $z = 5$ cm.